

# Detection of a Majorana fermion zero mode by a T-shaped quantum-dot structure

Wei-Jiang Gong,<sup>1</sup> Shu-Feng Zhang,<sup>2</sup> Zhi-Chao Li,<sup>1</sup> Guangyu Yi,<sup>1</sup> and Yi-Song Zheng<sup>3,\*</sup>

<sup>1</sup>College of Sciences, Northeastern University, Shenyang 110819, China

<sup>2</sup>Institute of Physics, Chinese Academy of Sciences, Beijing 100080, China

<sup>3</sup>Key Laboratory of Physics and Technology for Advanced Batteries, Ministry of Education, Department of Physics, Jilin University, Changchun 130023, China

(Received 27 August 2013; revised manuscript received 27 May 2014; published 10 June 2014)

We investigate the electron transport through the T-shaped quantum-dot (QD) structure theoretically, by coupling a Majorana zero mode to the terminal QD. It is found that in the double-QD configuration, the presence of the Majorana zero mode can efficiently dissolve the antiresonance point in the conductance spectrum while inducing a conductance peak to appear at the same energy position. In the case of asymmetric QD-lead coupling, such a valley-to-peak transition induced by the Majorana zero mode still exists. Next, we observe in the multi-QD case that at the zero-bias limit, the conductance values are always the same as the double-QD result, independent of the parity of the QD number. We believe that all these results can be helpful for understanding the properties of Majorana bound states.

DOI: [10.1103/PhysRevB.89.245413](https://doi.org/10.1103/PhysRevB.89.245413)

PACS number(s): 73.21.-b, 74.78.Na, 73.63.-b, 03.67.Lx

## I. INTRODUCTION

Majorana fermions, exotic quasiparticles with non-Abelian statistics, have attracted a great deal of attention due to both their fundamental interest and the potential application for the decoherence-free quantum computation. Different groups have proposed various ways to realize unpaired Majorana fermions, such as in a vortex core in a p-wave superconductor [1–6] or superfluid [7,8]. Recently, it has been reported that Majorana bound states (MBSs) can be realized at the ends of a one-dimensional p-wave superconductor for which the proposed system is a semiconductor nanowire with Rashba spin-orbit interaction to which both a magnetic field and proximity-induced s-wave pairing are added [9–12]. This means that Majorana fermions can be constructed in solid states, and that its application becomes more feasible. However, how to detect and verify the existence of MBSs is a key issue and is rather difficult. Various schemes have been suggested, including the noise measurements [13,14], the resonant Andreev reflection by a scanning tunneling microscope (STM) [15], and the  $4\pi$  periodic Majorana-Josephson currents [16].

More recently, some researchers demonstrated that the MBS can be detected by coupling it laterally to a QD in one closed circuit. The main reason arises from the quantifiable change of the MBS on the electron transport through a QD structure. For example, when the QD is noninteracting and in the resonant-tunneling regime, the MBS influences the conductance through the QD by inducing the sharp decrease of the conductance by a factor of  $\frac{1}{2}$ , as reported by D. E. Liu and H. U. Baranger [17]. If the QD is in the Kondo regime, the QD-MBS coupling reduces the unitary-limit value of the linear conductance by exactly a factor  $\frac{3}{4}$  [18]. These results exactly illustrate that the QD structure is a good candidate for the detection of MBSs. Motivated by these works, researchers tried to clarify the other underlying transport properties of the QD structure due to the QD-MBS coupling. Y. Cao *et al.* discussed the current and shot noise properties of this

system by tuning the structure parameters [19]. Besides, the MBS-assisted transport properties have been investigated in the double-QD structures, and a variety of interesting results have been observed, such as the crossed Andreev reflection [20] and nonlocal entanglement [21]. These works illustrated that it can be feasible to detect Majorana fermions in QD structures. However, MBS is not the necessary factor to quantitatively change the resonant tunneling, because various decoherence factors can suppress it. This means that it is less convincing to detect the MBSs by observing the change of resonant tunneling. Therefore, any new schemes to efficiently detect the MBSs are desirable.

QDs have one important characteristic in that some QDs can be coupled to form the coupled-QD systems. In comparison with the single-QD and double-QD systems, multiple QDs present more intricate quantum transport behaviors, because of the tunable structure parameters and abundant quantum interference mechanisms. As a typical example, the antiresonance in electronic transport through a T-shaped multi-QD structure were extensively studied in previous works [22–28]. Such an effect is tightly related to the parity of QD number. Namely, in the odd-numbered QD case, resonant tunneling occurs at the low-bias limit. Conversely, for the case of even-numbered QDs, the electronic transport shows the antiresonance effect which leads to one conductance zero [23,26]. In view of these results, it is natural to think that if the MBSs could efficiently modify the transport properties of the T-shaped QD structure, e.g., the antiresonance effect, such a QD structure will be a more promising candidate for the detection of MBSs. Motivated by this idea, in the present paper we consider a Majorana zero mode to side couple to the last QD of the T-shaped QD structure. By calculating the conductance spectrum, we found that the presence of the Majorana zero mode completely modifies the electron transport properties of the T-shaped QD structure. The conductance spectra always exhibit the similar conductance peaks whose values are equal to  $\frac{e^2}{2h}$  at the zero-bias limit, accompanied by the disappearance of the antiresonance effect. We therefore propose this structure to be an appropriate candidate to detect the MBSs.

\*zys@jlu.edu.cn

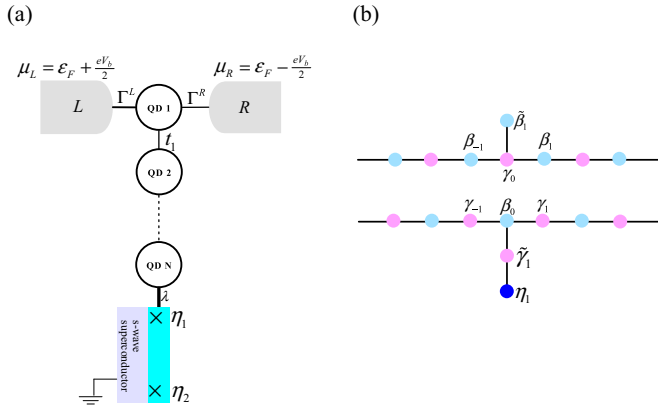


FIG. 1. (Color online) Sketch of a T-shaped QD system with coupled MBSs. The two MBSs are defined as  $\eta_1$  and  $\eta_2$ , respectively. The chemical potentials of the two normal leads are  $\mu_L = \epsilon_F + \frac{eV_b}{2}$  and  $\mu_R = \epsilon_F - \frac{eV_b}{2}$ . (b) Schematic of the T-shaped double-QD structure with coupled MBSs in the Majorana fermion representation.

## II. MODEL

The electronic transport structure we propose to detect the MBS is illustrated in Fig. 1(a). In such a structure, the last QD of a noninteracting T-shaped QD system is coupled to one MBS. With the current experimental technique, the T-shaped QD structure can be readily fabricated. And it is also actually possible to measure its electron transport spectrum. For example, the antiresonance phenomenon in the electron transport process has been successfully observed in a recent experimental work [25,29]. As for the realization of the MBSs, various schemes have been proposed. For instance, when a semiconductor nanowire with strong Rashba interaction is subjected to a strong magnetic field  $B$  and adheres to a grounded proximity-induced  $s$ -wave superconductivity, a pair of MBSs can form at the end of the nanowire [5,11], in the case of  $V_z = g\mu_B B/2 > \sqrt{\Delta^2 + \mu^2}$  ( $\Delta$  is the superconducting order parameter and  $\mu$  is the chemical potential of the nanowire).

In Fig. 1, one MBS, defined by  $\eta_1$ , is assumed to be coupled to QD- $N$ . Accordingly, the Hamiltonian of such a structure can be written as

$$H = H_0 + H_M + H_{MD}. \quad (1)$$

The first term is the Hamiltonian for the T-shaped QD system with the two connected normal metallic leads, which takes the form

$$H_0 = \sum_{\alpha k} \epsilon_{\alpha k} c_{\alpha k}^\dagger c_{\alpha k} + \sum_{j=1}^N \epsilon_j d_j^\dagger d_j + \sum_{j=1}^{N-1} t_j d_j^\dagger d_{j+1} + \sum_{\alpha k} V_\alpha d_1^\dagger c_{\alpha k} + \text{H.c.} \quad (2)$$

$c_{\alpha k}^\dagger$  ( $c_{\alpha k}$ ) is an operator to create (annihilate) an electron of the continuous state  $|k\rangle$  in the lead- $\alpha$  ( $\alpha \in L, R$ ).  $\epsilon_{\alpha k}$  is the corresponding single-particle energy.  $d_j^\dagger$  ( $d_j$ ) is the creation (annihilation) operator of the electron in QD- $j$ .  $\epsilon_j$  denotes the electron level in the corresponding QD.  $t_j$  denotes the tunneling between the two neighboring QDs.  $V_\alpha$  is the

tunneling element between QD-1 and lead- $\alpha$ . Note that since the QD structure is noninteracting, we in this paper neglect the spin index. Next, the low-energy effective Hamiltonian for  $H_M$  (i.e., the Majorana fermion) reads

$$H_M = i\epsilon_M \eta_1 \eta_2. \quad (3)$$

It describes the paired MBSs generated at the ends of the nanowire and coupled to each other by an energy  $\epsilon_M \sim e^{-l/\xi}$ , with  $l$  the wire length and  $\xi$  the superconducting coherent length. The last term in Eq. (1) describes the tunnel coupling between QD- $N$  and the nearby MBS, which is given by

$$H_{MD} = (\lambda d_N - \lambda^* d_N^\dagger) \eta_1. \quad (4)$$

$\lambda$  is the coupling coefficient between QD- $N$  and the MBS.

In Fig. 1(a), we know that  $\mu_L = \epsilon_F + \frac{eV_b}{2}$  and  $\mu_R = \epsilon_F - \frac{eV_b}{2}$  ( $\mu_\alpha$  is the chemical potential of lead- $\alpha$ , and  $\epsilon_F$  is the Fermi level in the case of  $V_b = 0$  which can be assumed to be zero), and their difference will drive the transport. In order to realize the robust MBSs, the following condition must be satisfied: the Zeeman splitting  $V_z \gg |V_b|$ ,  $\lambda$ , and  $\Gamma$ .  $\Gamma = \frac{1}{2}(\Gamma^L + \Gamma^R)$  is the QD-lead coupling with  $\Gamma^\alpha \equiv 2\pi |V_\alpha|^2 \rho$  and  $\rho$  the density of states of the leads. Note that in the presence of MBSs, this structure is actually a three-terminal system. Thus, the current of lead  $L$  and lead  $R$  should be calculated, respectively, for completely clarifying the transport properties. The current in lead  $\alpha$  can be evaluated by various methods, such as the scattering matrix method and the nonequilibrium Green function technique [20,30]. We here employ the latter to discuss the transport behaviors. Via a straightforward derivation, we obtain the expression of the current in one lead, e.g., lead  $L$ :

$$J_\alpha = \frac{e}{h} \int d\omega [T_{ee}^{\alpha\alpha'}(\omega)(f_e^\alpha - f_e^{\alpha'}) + T_{eh}^{\alpha\alpha}(\omega)(f_e^\alpha - f_h^\alpha)]. \quad (5)$$

In this formula,  $f_e^\alpha$  and  $f_h^\alpha$  are the Fermi distributions of the electron and hole in lead  $\alpha$ , respectively.  $T_{ee}^{\alpha\alpha'}(\omega) = \text{Tr}[\Gamma_e^\alpha \mathbf{G}^R \Gamma_e^{\alpha'} \mathbf{G}^A]$  and  $T_{eh}^{\alpha\alpha}(\omega) = \text{Tr}[\Gamma_e^\alpha \mathbf{G}^R \Gamma_h^\alpha \mathbf{G}^A]$ , where  $\mathbf{G}^R$  and  $\mathbf{G}^A$  are the related and advanced Green functions.

In order to get the analytical form of the retarded Green function, it is necessary to switch from the Majorana fermion representation to the completely equivalent regular fermion one by defining  $\eta_1 = (f^\dagger + f)/\sqrt{2}$  and  $\eta_2 = i(f^\dagger - f)/\sqrt{2}$  with  $\{f, f^\dagger\} = 1$ . Accordingly, we can write out  $H_M$  and  $H_D$ , respectively, as  $H_M = \epsilon_M (f^\dagger f - \frac{1}{2})$  and

$$H_{MD} = \frac{1}{\sqrt{2}} (\lambda d_N - \lambda^* d_N^\dagger) (f^\dagger + f). \quad (6)$$

Then with the equation of motion method, the matrix form of the retarded Green function can be written out, i.e.,

$$\mathbf{G}^R(\omega) = \begin{bmatrix} g_1(z)^{-1} & 0 & -t_1 & 0 & 0 & 0 & 0 & \cdots & 0 \\ 0 & \tilde{g}_1(z)^{-1} & 0 & t_1 & 0 & 0 & 0 & \cdots & 0 \\ -t_1^* & 0 & g_2(z)^{-1} & 0 & -t_2 & 0 & 0 & \cdots & 0 \\ 0 & t_1^* & 0 & \tilde{g}_2(z)^{-1} & 0 & \ddots & 0 & \cdots & \vdots \\ 0 & 0 & -t_2^* & 0 & \ddots & 0 & t_{N-1} & \cdots & \vdots \\ 0 & 0 & & \ddots & 0 & g_N(z)^{-1} & 0 & \frac{\lambda^*}{\sqrt{2}} & \frac{\lambda^*}{\sqrt{2}} \\ \vdots & & & & t_{N-1}^* & 0 & \tilde{g}_N(z)^{-1} & -\frac{\lambda}{\sqrt{2}} & -\frac{\lambda}{\sqrt{2}} \\ 0 & 0 & \cdots & 0 & 0 & \frac{\lambda}{\sqrt{2}} & -\frac{\lambda^*}{\sqrt{2}} & g_M(z)^{-1} & 0 \\ 0 & 0 & 0 & 0 & \cdots & \frac{\lambda}{\sqrt{2}} & -\frac{\lambda^*}{\sqrt{2}} & 0 & \tilde{g}_M(z)^{-1} \end{bmatrix}^{-1}. \quad (7)$$

In the above equation,  $g_j(z)^{-1} = \omega - \varepsilon_j + i\Gamma\delta_{j1}$  and  $\tilde{g}_j(z)^{-1} = \omega + \varepsilon_j + i\Gamma\delta_{j1}$ ;  $g_M(z)^{-1} = \omega - \varepsilon_M + i0^+$  and  $\tilde{g}_M(z)^{-1} = \omega + \varepsilon_M + i0^+$ . Within the wide-band limit approximation,  $\Gamma_e^\alpha = \Gamma_h^\alpha = \Gamma^\alpha$ . Moreover, in the symmetric-coupling case where  $\Gamma^\alpha = \Gamma$ , we can simplify the current formula in this structure as

$$J = \frac{e}{h} \int d\omega T(\omega)(f_e^L - f_e^R), \quad (8)$$

in which  $T(\omega) = -\Gamma \text{Im}G_{11}^R$ .

### III. NUMERICAL RESULTS AND DISCUSSIONS

With the formulation developed in the above section, we perform the numerical calculation to investigate the electron transport properties of the T-shaped QD structure. In the context, temperature is fixed at  $k_B T = 0$ . For the unit of the structure parameters, it is reasonable to consider it to be  $10^{-2}$  meV according to the previous works [20]. In the following, we ignore the unit of the parameters for simplicity.

First of all, we investigate the electron transport properties of the double-QD configuration with the finite coupling between QD-2 and  $\eta_1$ . The numerical results are shown in Fig. 2, where  $\varepsilon_j$  is taken to be zero. In Fig. 2(a), we find that in the case of  $\lambda = 0$ , the conductance exhibits two peaks at the points of  $eV_b = \pm 2.0$ , and at the point of  $eV_b = 0$  it becomes equal to zero. These two results are easy to understand. In the case of  $\varepsilon_j = 0$ , the molecular states of the double QDs are located at the points of  $\omega = \pm t_1$ . When  $eV_b = \pm 2.0$ , the Fermi levels of the leads will coincide with the energy levels of the molecular states, respectively. On the other hand, many groups have demonstrated that such a structure provides two special transmission paths for the quantum interference. As a result, when the energy of the incident electron is the same as the energy level of the side-coupled QD, destructive quantum interference will take place, leading to the well-known Fano antiresonance effect. In the zero-bias limit, only the zero-energy electron takes part in the quantum transport, so the conductance zero comes into being.

Next, when the coupling between QD-2 and  $\eta_1$  is incorporated, we can clearly find that the conductance peaks are first suppressed and then split. What is interesting is that in

the presence of nonzero  $\lambda$ , the conductance at the zero-bias point shows a peak. By a further observation, we know that the conductance value at the energy zero point is exactly equal to  $e^2/2h$ . With the enhancement of such a coupling, this conductance peak is widened, leaving its peak height unchanged. To explain this result, we should first solve the value of the conductance peak mathematically. Based on the expression of  $\mathbf{G}^R$  in Eq. (7), we get the analytical form of  $G_{11}^R$

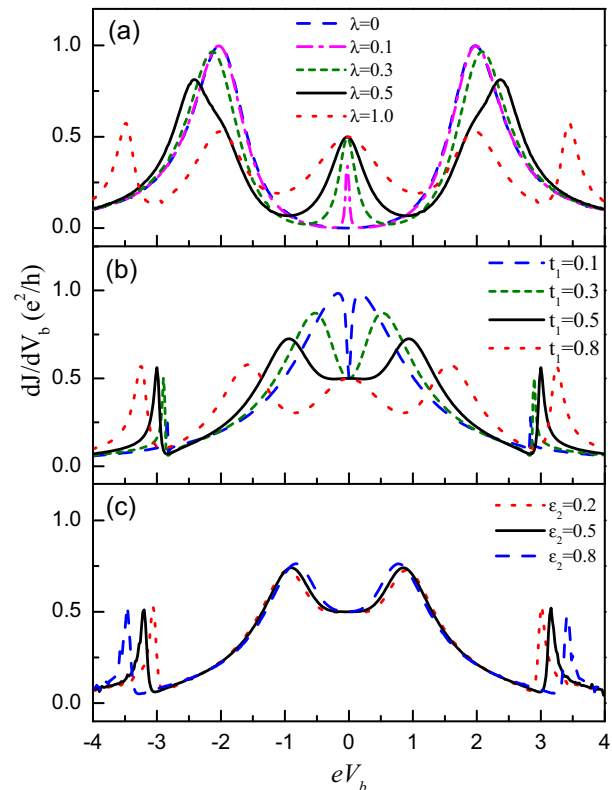


FIG. 2. (Color online) The conductance spectra of the T-shaped double-QD structure. The QD-lead coupling is fixed with  $\Gamma = 0.5$ . (a) The conductance as functions of  $eV_b$  with the increase of the coupling between QD-N and  $\eta_1$ . The interdot coupling is taken to be  $t_1 = 1.0$ . (b) The conductance as functions changed by the decrease of the interdot coupling,  $\lambda = 1.0$ . (c) The conductance influenced by the shift of  $\varepsilon_2$  with  $t_1 = 0.5$  and  $\lambda = 1.0$ .

in the finite- $\lambda$  case, i.e.,

$$G_{11}^R = 1/[\omega - \varepsilon_1 + i\Gamma - \frac{|t_1|^2 \Delta(\omega) - |t_1 \lambda|^2 \omega(\omega + \varepsilon_1 + i\Gamma)}{(\omega - \varepsilon_2) \Delta(\omega) + |t_1 \lambda|^2 \omega - 2|\lambda|^2 \omega^2 (\omega + \varepsilon_1 + i\Gamma)}], \quad (9)$$

where  $\Delta(\omega) = [(\omega + \varepsilon_1 + i\Gamma)(\omega + \varepsilon_2) - |t_1|^2](\omega^2 - \varepsilon_M^2)$ . Such a result shows that the nonzero  $\lambda$  indeed complicates the self energy of  $G_{11}^R$ , hence to modify its properties. It is known that in the case of  $V_b \rightarrow 0$ , the electron transport is in the linear regime where  $J = \mathcal{G} \cdot V_b$ . Here  $\mathcal{G}$  is the so-called linear conductance defined by  $\mathcal{G} = \frac{e^2}{h} T(\omega)|_{\omega=0}$ . Surely, in such a case, the characteristic of  $G_{11}^R$  in the region of  $\omega \rightarrow 0$  plays a dominant role in contributing to the linear conductance. We can readily find that in the case of  $\omega \rightarrow 0$ ,  $G_{11}^R$  can be simplified, i.e.,  $G_{11}^R \approx \frac{1}{\omega + 2i\Gamma}$ . Accordingly, the conductance is equal to  $\frac{e^2}{2h}$  in the zero-bias limit.

In order to further analyze the results shown in Fig. 2(a), we should clarify the underlying physics mechanism in such a structure. For this purpose, we rewrite the Hamiltonian in Eq. (1) in the Majorana representation. To be specific, the two leads should be first rewritten into two semi-infinite tight-binding fermionic chains, i.e.,  $\sum_k \varepsilon_{Lk} c_{Lk}^\dagger c_{Lk} = \sum_{j=-\infty}^{-1} \tau (c_j^\dagger c_{j-1} + \text{H.c.})$  and  $\sum_k \varepsilon_{Rk} c_{Rk}^\dagger c_{Rk} = \sum_{j=1}^{\infty} \tau (c_j^\dagger c_{j+1} + \text{H.c.})$  ( $\varepsilon_{\alpha k}$  and  $\tau$  are confined by the relation of  $\varepsilon_{\alpha k} = 2\tau \cos k$ ). Suppose  $d_1 = c_0$  ( $d_1^\dagger = c_0^\dagger$ ), i.e., the two leads with their connected QD-1 just becomes a one-dimensional chain. Next, by defining  $\beta_j = (c_j^\dagger + c_j)/\sqrt{2}$  and  $\gamma_j = i(c_j^\dagger - c_j)/\sqrt{2}$ , the one-dimensional chain reduces to two decoupled Majorana chains. By the same token, the side-coupled QD can be transformed into MBSs by defining  $\tilde{\beta}_1 = (d_1^\dagger + d_2)/\sqrt{2}$  and  $\tilde{\gamma}_1 = i(d_1^\dagger - d_2)/\sqrt{2}$ . One can find that the T-shaped double-QD structure can exactly be divided into two isolated T-shaped Majorana chains, as shown in Fig. 1(b). The difference between these two chains is that in the lower branch two MBSs couple to each other serially, whereas in the upper branch only one MBS exists. For each branch, the Majorana fermion transport can be evaluated by means of the nonequilibrium Green function technique. Since the calculation is simple, we would not like to present the detailed derivation process. As a result, we find that the T-shaped Majorana chain exhibits the same transport properties as the regular fermionic one. Namely, when the number of the side-coupled MBSs is odd, the transport spectra show up as an antiresonance point at the point of  $\omega = 0$ ; instead, the transport will be resonant if the MBS number is even. Therefore, in the T-shaped double-QD structure with the side-coupled MBSs, the transport is only contributed by the lower branch, which causes the value of the conductance to be equal to  $\frac{e^2}{2h}$  in the zero-bias limit.

Figure 2(b) shows the influence of changing  $t_1$  on the conductance properties. In this figure, we see that with the decrease of  $t_1$ , the conductance peaks in the vicinities of  $eV_b = \pm 1.5$  enhance and shift to the zero-bias direction. However, the conductance value at the zero-bias point is robust with  $\mathcal{G} \equiv \frac{e^2}{2h}$ . Thereby, at such a point the original conductance peak vanishes and a conductance valley forms. In addition, it can be seen that during the process of decreasing  $t_1$ , the

conductance peaks around the points of  $eV_b = \pm 3.0$  disappear. These results can be understood as follows. When  $t_1$  deceases, QD-2 tends to decouple from QD-1. In such a case, the strong coupling between QD-2 and  $\eta_1$  will construct a new MBS which couples to QD-1 weakly. Just due to this reason, we can find that the result of  $t_1 = 0.1$  is consistent with that of the small  $\lambda$  in Ref. [17].

In Fig. 2(c) we investigate the contribution of the shifted  $\varepsilon_2$  to the conductance result. We find that the conductance spectrum is nearly independent of the shift of  $\varepsilon_2$ . Especially in the zero-bias limit, the conductance value is always equal to  $\frac{e^2}{2h}$ . This result is completely opposite to that in the zero-MBS case where the antiresonance position is related to  $\varepsilon_2$ . We would like to analyze this result as follows. To start with, we can observe from Eq.(9) that in the case of  $\omega \rightarrow 0$ , the terms that include  $\varepsilon_2$  disappear. This means the trivial role of  $\varepsilon_2$  in the low-bias region. For the underlying physical picture, we can also clarify it in the Majorana representation. Surely, the nonzero  $\varepsilon_2$  contributes to the coupling between the two Majorana chains because a new term  $i\varepsilon_2 \tilde{\beta}_1 \tilde{\gamma}_1$  will be involved in the Hamiltonian if  $\varepsilon_2 \neq 0$ . Such a coupling will drive the finite transport between the two chains. According to the Landauer-Büttiker formula, the interchain transport ability is proportional to  $|\langle \tilde{\beta}_0 | \tilde{\gamma}_0 \rangle|^2$  ( $\langle \tilde{\beta}_0 | \tilde{\gamma}_0 \rangle$ ), the Green function between sites  $\tilde{\beta}_0$  and  $\tilde{\gamma}_0$ , reflects the interchain motion of the quasiparticle). By calculation, we see that  $\langle \tilde{\beta}_0 | \tilde{\gamma}_0 \rangle = i \frac{(\omega + i0^+) \varepsilon_2 t_1^2}{\det[\mathbf{G}^{-1}]}$  is dependent on  $\varepsilon_2$ ,  $\omega$ , and  $t_1$  ( $\mathbf{G}$  is the Green function matrix). It is obvious that in the low-bias limit,  $\langle \tilde{\beta}_0 | \tilde{\gamma}_0 \rangle$  will be equal to zero, irrelevant to the nonzero  $\varepsilon_2$ . As a result, the interchain transport vanish. The underlying physics can be clarified by analyzing the expression of  $\langle \tilde{\beta}_0 | \tilde{\gamma}_0 \rangle$ . We can readily find that  $\omega + i0^+$  is exactly the reciprocal of the Green function of the Majorana zero mode when  $\lambda = 0$ . This result means that  $\eta_1$  is a dangling state in the Majorana Fermion chain even in the case that the inter-chain coupling is established. The dangling  $\eta_1$  state plays the same role as a QD side coupling to an electronic transport structure to give rise to the conductance zero point when the incident electronic energy is equal to the energy level of the dangling state [22,24]. Based on this result, we readily know that in the presence of MBSs, the fluctuation of QD levels can not influence the electron transport in the low-bias limit, which is helpful for the relevant experiment.

We have to notice that in experiment, the QD-lead coupling may not be the same. It is necessary to investigate the case of asymmetric QD-lead coupling. Some previous works have discussed the transport behaviors in the single-QD structure when  $\Gamma^L \neq \Gamma^R$ . They found that in such a case, the currents in the two normal leads are different, because of the different-strength Andreev reflections from the MBS to the two normal leads. Also, by connecting the three terminals in one closed circuit, the current in the terminal with MBSs can be investigated [19]. However, even when  $\Gamma^L \neq \Gamma^R$ , it is feasible to use Eq. (5) to evaluate the current in lead- $\alpha$ . This can be proved by the scattering matrix method [20]. The reason is that the role of the third terminal in Fig. 1(a) is only to provide a pair of MBSs to affect the quantum transport. In Fig. 3, we take  $\Gamma^R = 0.5$  and calculate the conductance spectra. It can be found that in the absence of MBSs, the conductance magnitudes in the two terminals are the same,

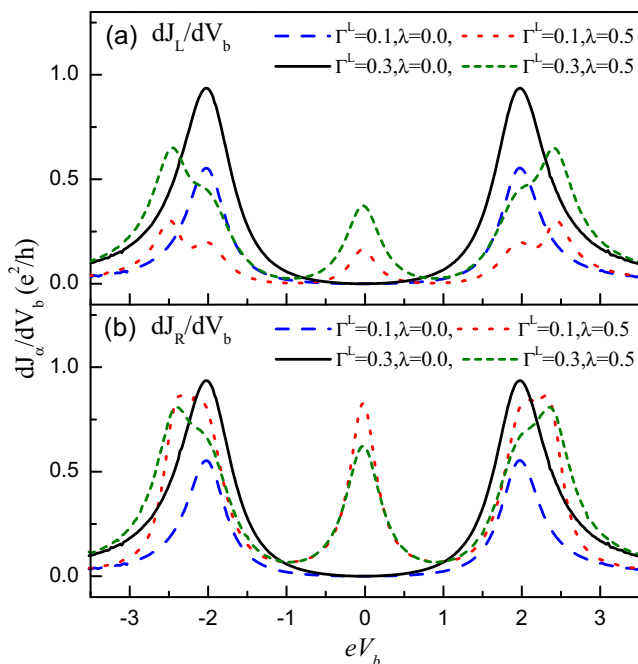


FIG. 3. (Color online) The conductances in lead  $L$  and lead  $R$  in the cases of asymmetric QD-lead coupling. The parameters are taken to be  $\epsilon_j = 0$ ,  $\Gamma^R = 0.5$ , and  $t_1 = 1.0$ .

which decrease with the decrease of  $\Gamma^L$ . What is important is that the antiresonance point at the zero-bias limit is robust, irrelevant to the change of conductance magnitude. When the MBS is introduced, the conductance results in the two terminals become different from each other. Namely, in lead  $L$  the zero-bias conductance peak weakens with the decrease of  $\Gamma^L$ , but for  $\frac{dJ_R}{dV_b}$ , such a peak is obviously enhanced. This result is easy to understand. Decreasing  $\Gamma^L$  weakens the Andreev reflection in lead- $L$  but strengthens that in lead- $R$ , leading to the different conductances in the two terminals. In spite of the conductance difference, the valley-to-peak transition induced by the MBSs can still be observed in the case of asymmetric QD-lead coupling. Up to now, we know that in this structure, the detection of the MBS is independent of the QD-lead coupling manner.

If the MBS wire is not long enough, the two MBSs will be coupled to each other. In Fig. 4 we present the conductance spectra in the case of nonzero coupling between the two MBSs. It can be found that different from the results of  $\epsilon_M = 0$ , the nonzero  $\epsilon_M$  induces the appearance of the conductance dip in the zero-bias limit. When  $\epsilon_M = 0.02$ , the conductance dip is relatively weak, and the conductance spectrum is consistent with that in the case of  $\epsilon_M = 0$  in principle. Next, with the increase of  $\epsilon_M$ , the conductance dip becomes apparent. Especially in the case of  $\epsilon_M = 0.3$ , it exactly becomes an antiresonance with the wide antiresonance valley. Similar results can be observed in the case of asymmetric QD-lead coupling [see Fig. 4(b)]. These results indicate that in the case of  $\epsilon_M \neq 0$ , the conductance spectrum will exhibit an antiresonance point at the zero-bias limit, similar to the zero-MBS result. Regardless of the splitting of the conductance peak at the zero-bias case, the height of the two new conductance

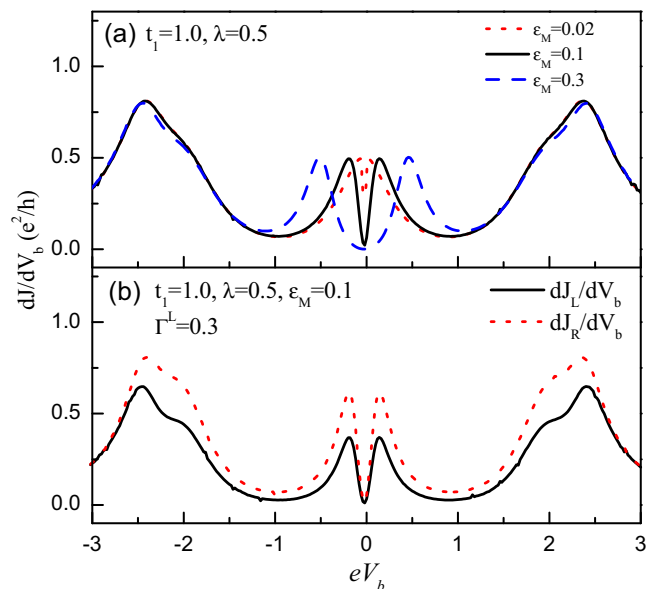


FIG. 4. (Color online) The conductance spectra of the T-shaped double-QD structure in the case of nonzero coupling between  $\eta_1$  and  $\eta_2$ .

peaks near the point of  $V_b = 0$  is the same as that in the case of  $\epsilon_M = 0$ . Therefore, even not in the zero mode, the effect of the QD-MBS coupling on the conductance is distinct.

We next calculate the electron transport by writing the MBS into a one-dimensional semi-infinite topological superconductor to check the robustness of the MBS signature in the real physical system [31]. For simplicity, we write  $H_M$  as a semi-infinite p-wave superconducting chain, i.e.,  $H_M = -\mu \sum_j c_j^\dagger c_j + \sum_j [t c_j^\dagger c_{j+1} + \Delta e^{i\phi} c_j^\dagger c_{j+1}^\dagger + \text{H.c.}]$ . Meanwhile,  $H_{MD}$  has its new expression:  $H_{MD} = t_d (d_2^\dagger c_1 + \text{H.c.})$ . By iteratively solving the end states of the chain, the MBS-assisted electron transport can be evaluated, and the influence of the structure parameters of  $H_M$  can be clarified, as shown in Fig. 5. In Fig. 5(a), we see that in the case of  $\Delta = 0$ , the conductance spectra are still characterized by the apparent valleys, despite the disappearance of the antiresonance. The reason is that in such a case, the superconductor just becomes a normal electron reservoir and introduces the inelastic scattering for electron transmission, hence to weaken the antiresonance effect. In the case of  $t_d = 0.2$ , the coupling between QD-2 and the chain is relatively weak, so the conductance minimum is almost equal to zero. In Fig. 5(b) when  $\Delta = 0.3$ , one conductance peak with its value equal to  $\frac{e^2}{2h}$  appears in the conductance spectra at the zero-bias limit. The decrease of  $t_d$  can only narrow the conductance peak but can not suppress its height. Similar results can be found in the process of increasing  $t$ , as shown in Fig. 5(c). In Fig. 5(d), we introduce the fluctuation of  $t$  and  $\Delta$  to check the conductance change. As reported by previous literature, structural disorder can modify the properties of MBSs [32]. It can be seen that the increase of fluctuation only narrows the width of the conductance peak, whereas the conductance value at the zero-bias limit does not change. The reason is that in the semi-infinite chain, the fluctuation of

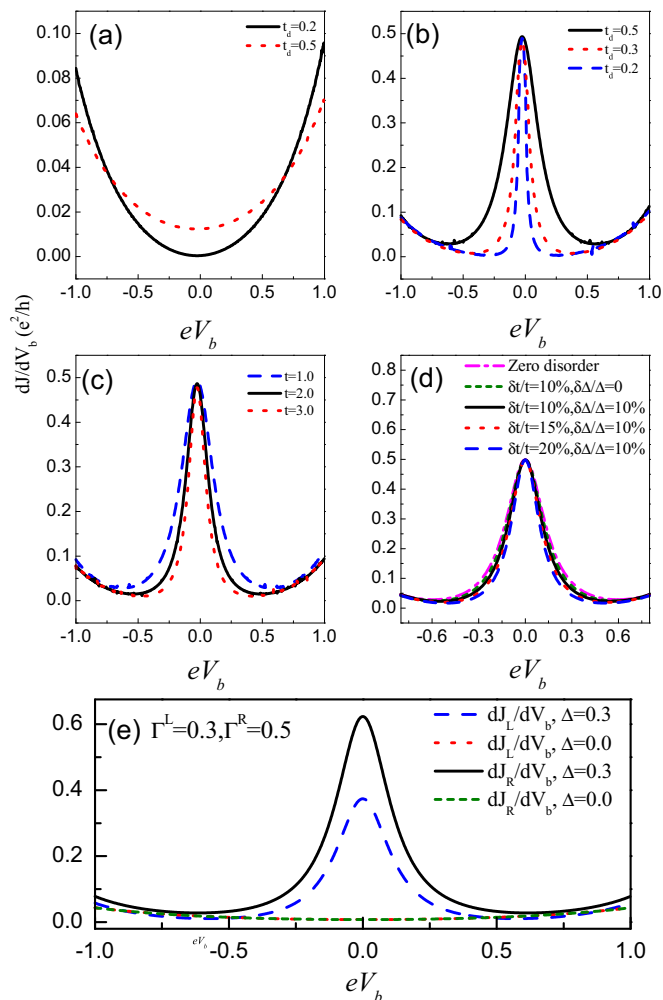


FIG. 5. (Color online) The influence of the Majorana zero mode on the electron transport in the double-QD case when the Majorana zero mode is mimicked by a semi-infinite chain. The structure parameters are taken as follows: (a)  $t = 1.0$  and  $\Delta = 0$ ; (b)  $t = 1.0$  and  $\Delta = 0.3$ ; (c)  $t_d = 0.5$  and  $\Delta = 0.3$ . (d)-(e) The conductance in the cases of fluctuated parameters and asymmetric QD-lead coupling. The parameters are taken to be  $t = 1.0$ ,  $\Delta = 0.3$ , and  $t_d = 0.5$ .

the structure parameters can only narrow the energy gap for the occurrence of MBS but can not remove it. In the following, the results in Fig. 5(e) can examine the results in Fig. 3. Namely, in the case of asymmetric QD-lead coupling, the valley-to-peak transition induced by the MBS holds. Note that when  $\Delta = 0$ , the semi-infinite chain is just a normal terminal. In such a case, we assume this terminal to be a floating lead (i.e., a voltage probe) with zero net current in it [33].

Motivated by the results of the double-QD structure, we next investigate the multi-QD case. According to the previous works, the antiresonance is tightly related to the QD number in the T-shaped multi-QD structure. Concretely, when the QD number is even, antiresonance always appear at the zero-bias point; the resonant tunneling will be observed at such a point otherwise [26,28]. In Fig. 6 we take the cases of  $N = 3$  and  $N = 4$  to compare the electron transport properties modified by the MBS in the T-shaped multi-QD structure. The relevant parameters are taken to be  $\varepsilon_j = 0$  and  $t_j = 1.0$ . From Fig. 6(a),

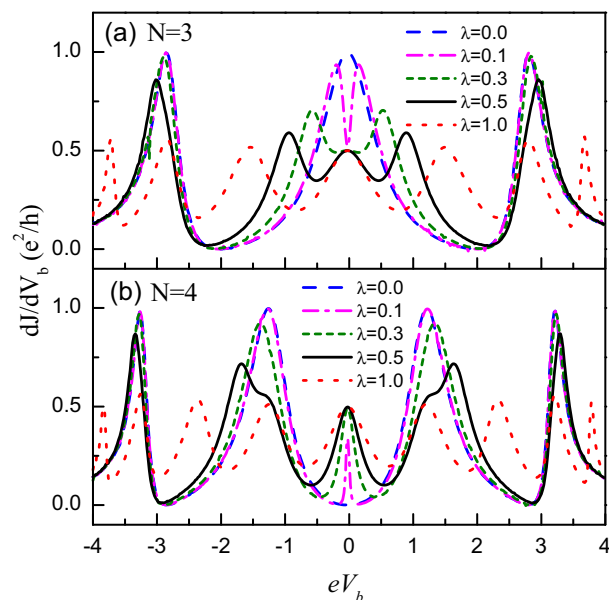


FIG. 6. (Color online) The conductance spectra of the T-shaped multi-QD structure. In (a)  $N = 3$ , and  $N = 4$  in (b). The relevant parameters are the same as those in Fig. 2.

we readily find that in the case of  $N = 3$ , the conductance is equal to  $\frac{e^2}{h}$  around the point of  $eV_b = 0$  when  $\lambda = 0$ . When  $\lambda = 0.1$ , despite the weak coupling between QD-3 and  $\eta_1$ , the conductance gradually decreases to  $\frac{e^2}{2h}$  at the zero-bias point. Consequently, the conductance exhibits a valley around the zero-bias point. With the increase of  $\lambda$ , such a valley becomes widened. When  $\lambda$  further increases to  $\lambda = 0.5$ , the conductance magnitude is suppressed apparently, leading to the formation of the conductance peak at the zero-bias point. Such a change process is similar to that in the single-QD case [17]. As for the results in Fig. 6(b) where  $N = 4$ , we see that they are similar to those in the double-QD case. The only difference is the increase of the conductance peaks. These results can be understood by following our analysis about the double-QD case. In the Majorana fermion representation, the T-shaped QD structure transforms into two isolated branches, and the side-coupled MBSs in the two branches just differ by one. Thus when the transport in one branch is resonant, the antiresonant transport certainly happens in the other. Therefore, in the low-bias limit, the conductance is certainly equal to  $\frac{e^2}{2h}$ , independent of the size of the side-coupled QD chain.

In the multi-QD structure, the nonuniformity of the QD levels and interdot couplings may be unavoidable in experiment. It is necessary to investigate the influences of the fluctuated QD levels or interdot couplings on the conductance. The corresponding results are shown in Figs. 7(a) and 7(b) for the triple-QD case and Figs. 7(c) and 7(d) for the four-QD structure. Here we choose  $\Gamma^\alpha = 0.5$  and  $\lambda = 0.5$ . It is not difficult to find that the change of the conductance spectra is not sensitive to the parameter disorder, though it almost reaches 20% [e.g., Fig. 7(d)]. Moreover, at the zero-bias limit, the conductance values are always equal to  $\frac{e^2}{2h}$ . We would like to analyze this result in the Majorana representation, similar to that about Fig. 2(c). We notice

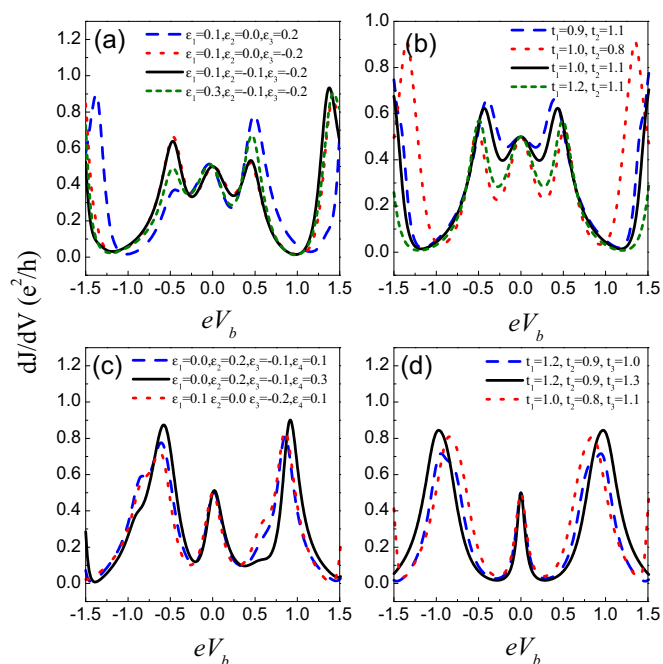


FIG. 7. (Color online) (a) The triple-QD conductance spectra in the case of the fluctuated QD levels. (b) The triple-QD conductance when the fluctuated interdot couplings is taken into account. (c),(d) The conductance spectra of the four-QD structure with the fluctuated QD levels and interdot couplings.

that the fluctuation of  $\epsilon_j$  can cause the interchain coupling, and the strength of such a coupling can be described by the value of  $|\langle\langle\beta_0|\tilde{\gamma}_0\rangle\rangle|^2$ . Our calculation shows that in the limit of  $\omega \rightarrow 0$ ,  $\langle\langle\beta_0|\tilde{\gamma}_0\rangle\rangle$  is proportional to  $(\omega + i0^+)$ , independent of the change of the QD number. Thus, in the zero-bias limit, the interchain transmission is always suppressed, whereas only the intrachain transmissions contribute to the conductance. For the fluctuation of  $t_j$ , it only changes the intersite hopping within one Majorana chain without destroying the structure of the two isolated Majorana chains. Therefore, in the presence of parameter disorder, the transports in two isolated Majorana chains remain and the zero-bias conductance value is unchanged. It should be emphasized that the above two results are actually irrelevant to the fluctuation strength. Namely, the uniform structural parameters of the QD chain are not the necessary condition for detecting the Majorana zero mode in experiment. This increases the feasibility of this scheme in experiment. In addition to the above results, we observe that in the four-QD case, the profile of the conductance peak around the zero-bias point is weakly dependent on the fluctuation of the QD levels or interdot couplings. The reason is that in the four-QD case, the conductance peak induced by the MBS-QD coupling appears in the conductance valley of the MBS-absent structure. When the MBS-QD coupling is relatively weak, the MBS couples weakly to the QD molecule states, so the zero-bias peak is insensitive to the fluctuation of the QD parameters. Such a result further proves the advantage of the valley-to-peak transition in detecting the Majorana zero mode. Except the above results, we find in Figs. 7(a) and 7(c) that the conductance spectra present the electron-hole asymmetry. This result is exactly induced by the fluctuation of the QD

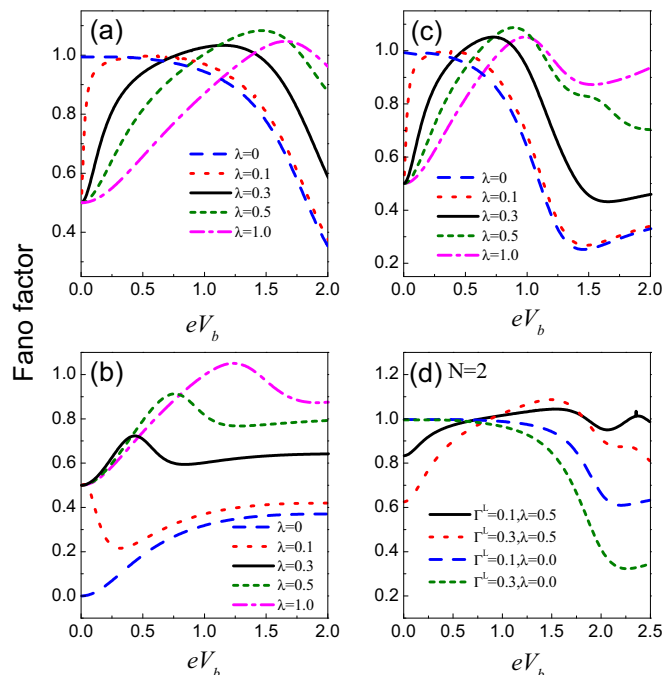


FIG. 8. (Color online) The Fano-factor spectra of the T-shaped QD structure. (a)  $N = 2$ ; (b)  $N = 3$ ; (c)  $N = 4$ . The relevant parameters are the same as those in Fig. 2(a). (d) The Fano factor in the  $N = 2$  case of asymmetric QD-lead coupling.

levels, and it can be explained as follows. The conductance is contributed by the local Andreev reflection and the interlead tunneling. When QD levels depart from the energy zero point, the electron-hole asymmetry appears in the process of the interlead tunneling [34]. Therefore, the conductance spectra show the electron-hole asymmetry.

Due to the presence of the MBSs, the noise properties will be changed. We would like to investigate the noise of such a kind of structure based on the theory in the previous works [12,20]. The results of the Fano factor of the configuration of  $N = 2, 3$ , and 4 are displayed in Fig. 8. In Fig. 8(a) where  $N = 2$ , we plot the spectra of the Fano factor by increasing the coupling between QD-2 and  $\eta_1$ . It is easy to find that in the zero-bias limit, when  $\lambda = 0$ ,  $\gamma_0$  is equal to 1, but a nonzero  $\lambda$  can efficiently suppress the value of  $\gamma_0$  to be  $\frac{1}{2}$ . Next, the further increase of  $\lambda$  can not change this result. Such a phenomenon can be explained as follows. In the case of symmetric QD-lead coupling, the noise formula can be simplified substantially, i.e.,  $S(0) = \frac{2e^2}{h} \int d\omega T(\omega)[1 - T(\omega)](f_e^L - f_e^R)$ , which is the same as that in the two-terminal case. The Fano factor can then be defined as  $\gamma_0 = \frac{S(0)}{2eJ}$ . At the zero-bias limit,  $\gamma_0$  can be simplified as  $\gamma_0 = 1 - T(\omega = 0)$ . Surely, the antiresonance effect will make  $\gamma_0$  equal to 1.0 in the case of  $\lambda = 0$ . But when the nonzero  $\lambda$  is incorporated,  $T(\omega = 0) = \frac{1}{2}$ , which accordingly leads to the result of  $\gamma_0|_{eV_b=0} = \frac{1}{2}$ . In Fig. 8(b) where  $N = 3$ , we see that in the case of  $\lambda = 0$ ,  $\gamma_0 = 0$ , but the increment of  $\lambda$  causes  $\gamma_0$  to be equal to  $\frac{1}{2}$  at the zero-bias limit. It is certain that these results obey the relationship of  $\gamma_0 = 1 - T(\omega = 0)$ . In addition, the increase of  $\lambda$  enhances the amplitude of  $\gamma_0$ . The main cause should be attributed to the weakened transport in the presence of MBS-QD coupling.

Next, as shown in Fig. 8(c) where  $N = 4$ , the modification of the Fano factor is similar to that in the case of  $N = 2$ , in addition to the shift of the maximum of  $\gamma_0$  to the low-bias direction. In Fig. 8(d), we take the  $N = 2$  case to investigate the Fano factor under the condition of asymmetric QD-lead coupling. In the zero-bias limit, when  $\lambda = 0\gamma_0$  is also equal to 1, similar to that in the case of symmetric QD-lead coupling. When  $\lambda = 0.5$  the Fano factor is tightly dependent on the value of  $\Gamma^L$ . Besides, we can find that  $\gamma_0 \approx 1 - T(\omega = 0)$  in such a case, which is different from the result of a normal three-terminal structure [35].

#### IV. SUMMARY

In summary, we have introduced a Majorana zero mode to couple to the last QD of the T-shaped QD structure and then investigated the electron transport in it. After numerical calculation, we have found that the existence of the Majorana zero mode completely modifies the electron transport properties of the QD structure. For a typical structure of double QDs, the coupling between the Majorana zero mode and the side-coupled QD efficiently removes the antiresonance point in the conductance spectrum and induces a conductance peak to appear at the same energy position whose value is equal to  $\frac{e^2}{2h}$ . Such a result was checked by the tight-binding calculations. We believe that such an

antiresonance-resonance transformation will be more feasible to detect the MBSs, in comparison with the change of from  $\frac{e^2}{h}$  to  $\frac{e^2}{2h}$  in the single-QD structure. Next, the influences of the MBSs on the electron transport in the multi-QD structure have been discussed. It showed that the conductance spectra always exhibit the similar conductance peaks whose values are always equal to  $\frac{e^2}{2h}$  in the zero-bias limit, independent of the change of QD number. This result further confirms that such a kind of structure is fit for detecting the MBSs. By transforming the QD system into the Majorana fermion representation, all the results have been well clarified. In addition, the noise properties of this structure have been presented, which enrich the information of the MBS-assisted electron transport. We believe that this work can be helpful for the relevant experiments.

#### ACKNOWLEDGMENTS

This work was financially supported by the Natural Science Foundation of Liaoning province of China (Grant No. 2013020030), the Liaoning BaiQianWan Talents Program (Grant No. 2012921078), and the Fundamental Research Funds for the Central Universities (Grant No. N130505001). Y.-S.Z. was supported by the National Natural Science Foundation of China (Grants No. 11074091 and 91121011). W.-J.G. thanks B. H. Wu for helpful discussions.

- 
- [1] G. Moore and N. Read, *Nucl. Phys. B* **360**, 362 (1991).
  - [2] N. Read and D. Green, *Phys. Rev. B* **61**, 10267 (2000).
  - [3] L. Fu and C. L. Kane, *Phys. Rev. Lett.* **100**, 096407 (2008).
  - [4] M. Sato, Y. Takahashi, and S. Fujimoto, *Phys. Rev. Lett.* **103**, 020401 (2009).
  - [5] J. D. Sau, R. M. Lutchyn, S. Tewari, and S. Das Sarma, *Phys. Rev. Lett.* **104**, 040502 (2010).
  - [6] J. Alicea, *Phys. Rev. B* **81**, 125318 (2010).
  - [7] N. B. Kopnin and M. M. Salomaa, *Phys. Rev. B* **44**, 9667 (1991).
  - [8] S. Tewari, S. Das Sarma, C. Nayak, C. Zhang, and P. Zoller, *Phys. Rev. Lett.* **98**, 010506 (2007).
  - [9] A. Y. Kitaev, *Phys. Usp.* **44**, 131 (2001).
  - [10] R. M. Lutchyn, J. D. Sau, and S. Das Sarma, *Phys. Rev. Lett.* **105**, 077001 (2010).
  - [11] Y. Oreg, G. Refael, and F. von Oppen, *Phys. Rev. Lett.* **105**, 177002 (2010).
  - [12] B. H. Wu and J. C. Cao, *Phys. Rev. B* **85**, 085415 (2012).
  - [13] C. J. Bolech and E. Demler, *Phys. Rev. Lett.* **98**, 237002 (2007).
  - [14] J. Nilsson, A. R. Akhmerov, and C. W. J. Beenakker, *Phys. Rev. Lett.* **101**, 120403 (2008).
  - [15] K. T. Law, P. A. Lee, and T. K. Ng, *Phys. Rev. Lett.* **103**, 237001 (2009).
  - [16] L. Fu and C. L. Kane, *Phys. Rev. B* **79**, 161408 (2009).
  - [17] D. E. Liu and H. U. Baranger, *Phys. Rev. B* **84**, 201308(R) (2011).
  - [18] M. Lee, J. S. Lim, and R. López, *Phys. Rev. B* **87**, 241402(R) (2013).
  - [19] Y. Cao, P. Wang, G. Xiong, M. Gong, and X. Q. Li, *Phys. Rev. B* **86**, 115311 (2012).
  - [20] B. Zocher and B. Rosenow, *Phys. Rev. Lett.* **111**, 036802 (2013).
  - [21] Z. Wang, X. Y. Hu, Q. F. Liang, and X. Hu, *Phys. Rev. B* **87**, 214513 (2013).
  - [22] X. R. Wang, Yupeng Wang, and Z. Z. Sun, *Phys. Rev. B* **65**, 193402 (2002).
  - [23] P. A. Orellana, F. Domínguez-Adame, I. Gómez, and M. L. Ladrón de Guevara, *Phys. Rev. B* **67**, 085321 (2003).
  - [24] K. Kobayashi, H. Aikawa, A. Sano, S. Katsumoto, and Y. Iye, *Phys. Rev. B* **70**, 035319 (2004).
  - [25] M. Sato, H. Aikawa, K. Kobayashi, S. Katsumoto, and Y. Iye, *Phys. Rev. Lett.* **95**, 066801 (2005).
  - [26] Y. Zheng, T. Lü, C. Zhang, and W. Su, *Physica E (Amsterdam)* **24**, 290 (2004).
  - [27] M. E. Torio, K. Hallberg, S. Flach, A. E. Miroshnichenko, and M. Titov, *Eur. Phys. J. B* **37**, 399 (2004).
  - [28] Y. Liu, Y. Zheng, W. Gong, and T. Lü, *Phys. Lett. A* **360**, 154 (2006).
  - [29] S. Sasaki, H. Tamura, T. Akazaki, and T. Fujisawa, *Phys. Rev. Lett.* **103**, 266806 (2009).
  - [30] Y. Meir and N. S. Wingreen, *Phys. Rev. Lett.* **68**, 2512 (1992); W. Gong, Y. Zheng, Y. Liu, and T. Lü, *Phys. Rev. B* **73**, 245329 (2006).
  - [31] A. C. Potter and P. A. Lee, *Phys. Rev. Lett.* **105**, 227003 (2010).
  - [32] P. A. Iosevich, P. M. Ostrovsky, and M. V. Feigelman, *Phys. Rev. B* **86**, 035441 (2012); D. Bagrets and A. Altland, *Phys. Rev. Lett.* **109**, 227005 (2012); D. I. Pikulin, J. P. Dahlhaus, M. Wimmer, H. Schomerus, and C. W. J. Beenakker, *New J. Phys.* **14**, 125011 (2012).
  - [33] S. Datta, *Electron Transport in Mesoscopic Systems* (Cambridge University Press, Cambridge, 1997).
  - [34] R. A. Žak and K. Flensberg, *Phys. Rev. B* **77**, 045329 (2008); A. Levchenko and A. Kamenev, *Phys. Rev. Lett.* **101**, 216806 (2008); T. S. Kim and S. Hershfield, *ibid.* **88**, 136601 (2002).
  - [35] D. Sánchez and R. López, *Phys. Rev. B* **71**, 035315 (2005).